Effects of Antibiotics and a Proto-Oncogene Homolog on Destruction of Protein Translocator SecY

Johna van Stelten, *et al.*

Science **325**, 753 (2009);
DOI: 10.1126/science.1172221

Science (print ISSN 0036-8075; online ISSN 1095-9203) is published weekly, except the last week in December, by the American Association for the Advancement of Science, 1200 New York Avenue NW, Washington, DC 20005.

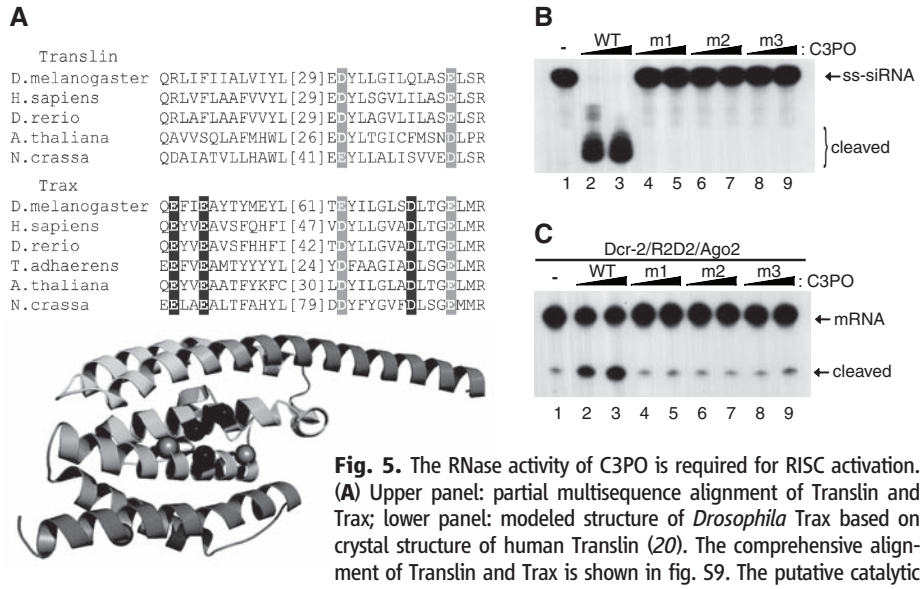

Fig. 5. The RNase activity of C3PO is required for RISC activation. (**A**) Upper panel: partial multisequence alignment of Translin and Trax; lower panel: modeled structure of *Drosophila* Trax based on crystal structure of human Translin (*20*). The comprehensive alignment of Translin and Trax is shown in fig. S9. The putative catalytic Asp and Glu residues are in black; two other highly conserved Glu residues are in gray. (**B**) RNase activity was compared between WT and each of three catalytic mutant C3PO complexes: m1 (Glu^{123} → Ala), m2 (Glu^{126} → Ala), and m3 (Asp^{204} → Ala). (**C**) RISC-enhancing activity was compared between WT and the three catalytic mutant C3PO complexes by assaying together with recombinant Dcr-2–R2D2 and Ago2.

References and Notes

1. R. W. Carthew, E. J. Sontheimer, *Cell* **136**, 642 (2009).
2. H. Siomi, M. C. Siomi, *Nature* **457**, 396 (2009).
3. Z. Paroo, Q. Liu, X. Wang, *Cell Res.* **17**, 187 (2007).
4. J. Liu *et al.*, *Science* **305**, 1437 (2004); published online 29 July 2004 (10.1126/science.1102513).
5. Q. Liu *et al.*, *Science* **301**, 1921 (2003).
6. J. W. Pham, J. L. Pellino, Y. S. Lee, R. W. Carthew, E. J. Sontheimer, *Cell* **117**, 83 (2004).
7. X. Liu, F. Jiang, S. Kalidas, D. Smith, Q. Liu, *RNA* **12**, 1514 (2006).
8. Y. Tomari, C. Matranga, B. Haley, N. Martinez, P. D. Zamore, *Science* **306**, 1377 (2004).
9. K. Okamura, A. Ishizuka, H. Siomi, M. C. Siomi, *Genes Dev.* **18**, 1655 (2004).
10. J. Wang, E. S. Boja, H. Oubrahim, P. B. Chock, *Biochemistry* **43**, 13424 (2004).
11. M. Claussen, R. Koch, Z. Y. Jin, B. Suter, *Genetics* **174**, 1337 (2006).
12. K. Suseendranathan *et al.*, *Eur. J. Cell Biol.* **86**, 173 (2007).
13. Y. Tomari *et al.*, *Cell* **116**, 831 (2004).
14. A. Nykanen, B. Haley, P. D. Zamore, *Cell* **107**, 309 (2001).
15. C. Matranga, Y. Tomari, C. Shin, D. P. Bartel, P. D. Zamore, *Cell* **123**, 607 (2005).
16. K. Miyoshi, H. Tsukumo, T. Nagami, H. Siomi, M. C. Siomi, *Genes Dev.* **19**, 2837 (2005).
17. T. A. Rand, S. Petersen, F. Du, X. Wang, *Cell* **123**, 621 (2005).
18. I. Sugiura *et al.*, *Acta Crystallogr.* **D60**, 674 (2004).
19. M. Maiti, H. C. Lee, Y. Liu, *Genes Dev.* **21**, 590 (2007).
20. Abbreviations for amino acid residues: A, Ala; C, Cys; D, Asp; E, Glu; F, Phe; G, Gly; H, His; I, Ile; K, Lys; L, Leu; M, Met; N, Asn; P, Pro; Q, Gln; R, Arg; S, Ser; T, Thr; V, Val; W, Trp; Y, Tyr.

21. We thank R. Koch, B. Suter, R. Carthew, M. Siomi, and H. Siomi for reagents and Y. Liu, H. Yu, D. Corey, and Z. Paroo for discussion and reading the manuscript. N.V.G. is a Howard Hughes Medical Institute investigator. Supported by a Sara and Frank McKnight fellowship (Y.L.), Welch grant I-1608 and NIH grant AG025688 (J.P.), and NIH grants GM078163 and GM084010 (Q.L.).

Supporting Online Material

www.sciencemag.org/cgi/content/full/325/5941/750/DC1
Materials and Methods
Figs. S1 to S10
References

14 May 2009; accepted 23 June 2009
10.1126/science.1176325

Effects of Antibiotics and a Proto-Oncogene Homolog on Destruction of Protein Translocator SecY

Johna van Stelten,[1] Filo Silva,[2] Dominique Belin,[2] Thomas J. Silhavy[1]*

Protein secretion occurs via translocation by the evolutionarily conserved Sec complex. LacZ hybrid proteins have long been used to study translocation in *Escherichia coli*. Some LacZ hybrids were thought to block secretion by physically jamming the Sec complex, leading to cell death. We found that jammed Sec complexes caused the degradation of essential translocator components by the protease FtsH. Increasing the amounts or the stability of the membrane protein YccA, a known inhibitor of FtsH, counteracted this destruction. Antibiotics that inhibit translation elongation also jammed the translocator and caused the degradation of translocator components, which may contribute to their effectiveness. Intriguingly, YccA is a functional homolog of the proto-oncogene product Bax Inhibitor-1, which may share a similar mechanism of action in regulating apoptosis upon prolonged secretion stress.

Protein translocation is a fundamental process that is essential for the delivery of most extracytoplasmic proteins to their final destination. This process is mediated by an evolutionarily conserved heterotrimeric membrane protein complex called the Sec61 complex (Sec61αβγ) in mammals and the Sec complex (SecY, -E, and -G) in prokaryotes (*1*). In *Escherichia coli*, two pathways target proteins to the Sec complex (*2*): the posttranslational Sec pathway, which targets most outer membrane (OM) and periplasmic proteins (*3*), and the cotranslational pathway, which is used primarily by inner membrane (IM) proteins, where the ribosome-nascent chain complex is targeted to the Sec complex by the signal recognition particle (SRP) (*4*). In both cases, proteins are initially directed to the SecY translocator via an amino-terminal signal sequence, which may or may not be cleaved upon translocation. The nature of this signal sequence determines which targeting pathway is used (*2*).

Genetic analysis of protein secretion is facilitated by *lacZ* (which specifies β-galactosidase) gene fusions (*5*, *6*). When the signal sequence of the OM protein LamB is fused to LacZ, the resulting hybrid protein is targeted for the posttranslational translocation pathway (*5*). Upon induction with maltose, large amounts of hybrid protein are made, and rapid folding of LacZ sequences in the cytoplasm causes a lethal jamming of the Sec complex (Fig. 1A), as evidenced by the accumulation in the cytoplasm of the precursor forms of wild-type secreted proteins (*7*). Under noninducing conditions (in the absence of maltose) in which low amounts of hybrid protein are made, lethal jamming does not occur. But because the hybrid protein is inefficiently secreted, some LacZ remains in the cytoplasm, where it is active, and strains carrying this fusion exhibit a Lac^+ phenotype. When the signal sequence of this hybrid is changed to increase its hydrophobicity, the resulting H*LamB-LacZ hybrid is directed instead to the alternative cotranslational SRP pathway (*4*). Because full-length LacZ is never exposed to the cytoplasm when secretion occurs cotranslationally, the H*LamB-LacZ hybrid is translocated efficiently to the periplasm, and jamming does not occur (Fig. 1B). In the oxidizing environment of the periplasm, LacZ misfolds. Thus, under noninducing conditions, strains carrying this fusion are Lac^-. Under inducing conditions, toxic hybrid protein aggregates accumulate in the periplasm so that even though no Sec complex jamming is observed, these strains are as maltose-sensitive as strains producing LamB-LacZ (*4*).

The Cpx two-component system regulates gene expression in response to misfolded proteins in the cell envelope. Dominant mutations, called *cpxA**, ac-

[1]Department of Molecular Biology, Princeton University, Princeton, NJ 08544, USA. [2]Department of Pathology and Immunology, Faculty of Medicine, University of Geneva, Geneva, Switzerland.

*To whom correspondence should be addressed. E-mail: tsilhavy@princeton.edu

tivate this system and suppress the inducer-sensitivity caused by periplasmic LacZ aggregates (*8*). Suppression of this toxicity was due solely to the induction by the Cpx system of the periplasmic protease DegP. Indeed, increasing production of DegP by cloning the structural gene on a multi-copy plasmid suppresses toxicity caused by H*LamB-LacZ (*4*). The protease degrades the toxic periplasmic LacZ aggregates. Activation of the Cpx system also relieves the inducer-sensitive phenotype caused by LamB-LacZ (*7*). This was surprising because this hybrid protein exerts its toxic effects in the cytoplasm by jamming the Sec complex. Indeed, overproduction of DegP is necessary but not sufficient to relieve the toxicity caused by LamB-LacZ (*4*). Activation of the Cpx system by use of *cpxA** alleles results in the efficient translocation of LamB-LacZ to the periplasm, where it can then be degraded by DegP (*7*). This reduced LacZ activity in uninduced cells (Fig. 2). Apparently, a Cpx-inducible gene product(s) other than DegP facilitates translocation of LamB-LacZ.

To search for this Cpx-inducible factor(s), we utilized the uninduced Lac phenotype of LamB-LacZ strains. Under these conditions, artificially increasing the production of the relevant factor in fusion strains that are $cpxA^+$ should increase the efficiency of LamB-LacZ secretion and thus decrease LacZ activity. Alternatively, inactivating the Cpx-regulated gene responsible for the efficient secretion of LamB-LacZ in a strain carrying the *cpxA** allele should increase LacZ activity. We began by testing genes regulated by Cpx (*9*).

The *yccA* gene is regulated in a Cpx-dependent fashion (*9*, *10*), and we confirmed this with reverse transcription polymerase chain reaction (fig. S1) (*11*). Overexpression of *yccA* from an isopropyl-β-D-thiogalactopyranoside (IPTG)–inducible promoter with a construct integrated at the lambda attachment site in a $cpxA^+$ fusion strain reduced LacZ activity comparable with that seen in *cpxA** fusion strains (Fig. 2) (*11*). Conversely, deletion of *yccA* in the *cpxA** fusion strain caused a modest increase in LacZ activity. The fact that $yccA^-$ is not completely epistatic to *cpxA** indicates that there are other Cpx-regulated factors that function to enhance translocation. Here, we focused on YccA because its increased production is sufficient to relieve jamming.

When SecY is not in a complex with SecE and SecG, it is degraded by FtsH, an essential, adenosine 5′-triphosphate–dependent, membrane-bound protease (*12*). In a search for mutants in which SecY was stabilized, a mutant form of the IM protein YccA, which lacks eight amino acids in the amino-terminus, was identified (*13*). This mutant protein, YccA11, binds to FtsH, but unlike wild-type YccA it is resistant to FtsH-mediated degradation (*13*). We replaced the chromosomal copy of *yccA* with *yccA11* in a $cpxA^+$ *lamB-lacZ* fusion strain and found that YccA11 was even more effective than overexpressed wild-type YccA at reducing LacZ activity (Fig. 2). Thus, YccA and even more so YccA11 can apparently stimulate secretion of the LamB-LacZ hybrid protein under noninducing conditions.

It had long been thought that the toxicity caused by high-level production of LamB-LacZ was due to a physical "jamming" of the Sec complex (*7*, *8*). Our results suggested an alternative hypothesis; perhaps the cell responds to jamming by promoting the energy-dependent degradation of SecY by FtsH. Translocator destruction would also cause the accumulation of the precursor forms of secreted proteins and result ultimately in cell death. Induction caused the degradation of SecY in strains carrying LamB-LacZ (Fig. 3A) but not in strains carrying the LamBΔ60-LacZ fusion in which the signal sequence is deleted (Fig. 3B) (*11*). Moreover, this degradation was prevented by

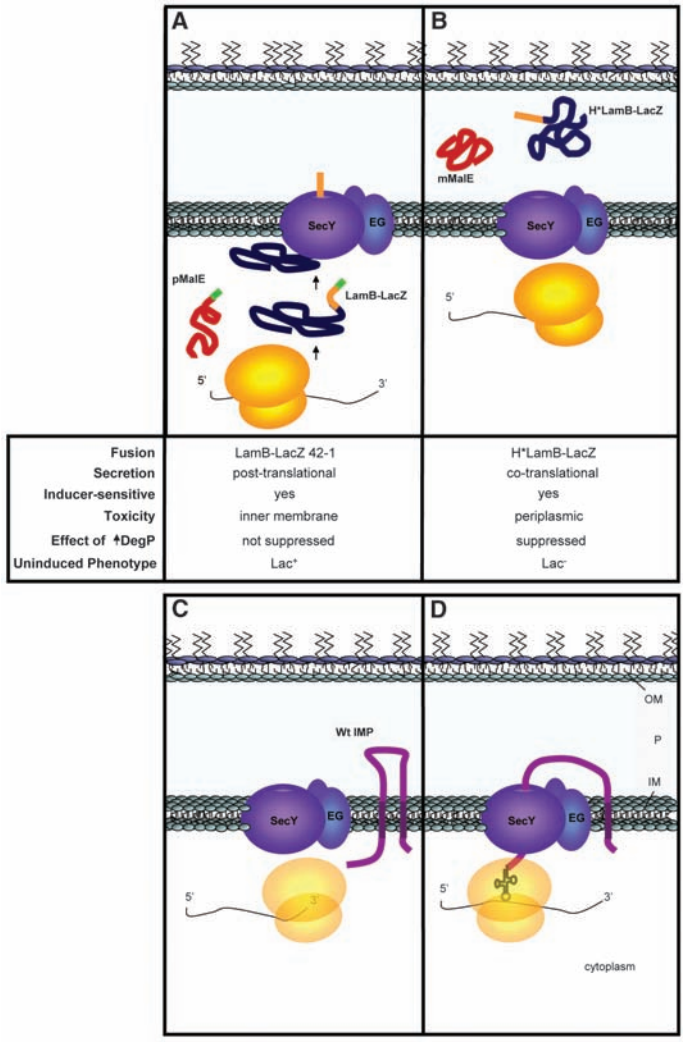

Fig. 1. Protein translocation in *E. coli*. (**A**) Jamming of SecY occurs during posttranslational translocation of the LamB-LacZ hybrid, resulting in accumulation of precursor proteins such as pMalE (red) with their signal sequence (green) still attached. (**B**) When the hybrid is targeted for cotranslational translocation (H*LamB-LacZ), it is secreted into the periplasm. Properties of the LacZ fusion strains are summarized in the text box. (**C**) Cotranslational translocation of a wild-type SRP substrate (purple). (**D**) During cotranslational translocation, antibiotics that inhibit peptide chain elongation jam the translocator. Orange circles, translating ribosome; IMP, IM protein; P, periplasm.

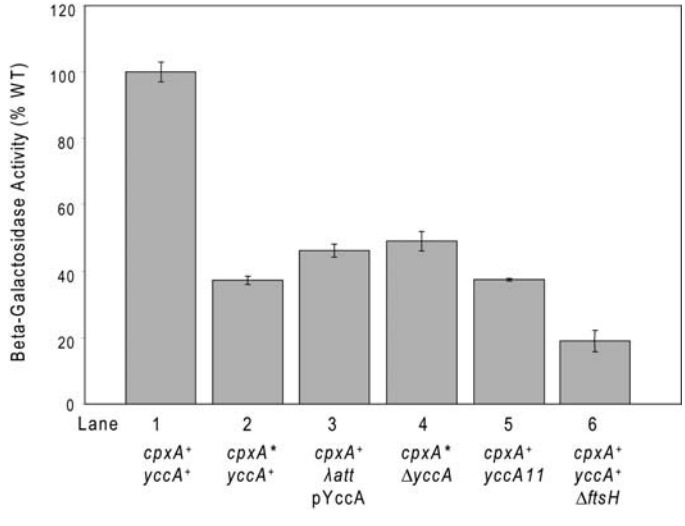

Fig. 2. YccA affects translocation of LamB-LacZ. Shown is LacZ activity of *lamB-lacZ* strains assayed in the absence of maltose induction so as to determine the efficiency of translocation. Lane 1, Pop3186 ($cpxA^+$ $yccA^+$); lane 2, WBS226 (*cpxA** $yccA^+$); lane 3, JVS724 ($cpxA^+$ λ*att* pYccA); lane 4, JVS621 (*cpxA** Δ*yccA*); lane 5, JVS716 ($cpxA^+$ *yccA*11); lane 6, JVS679 ($cpxA^+$ $yccA^+$ Δ*ftsH*). See table S1 for complete genotypes. Activities are expressed as a percent of wild type (WT). Error bars indicate SD (n = 3 experiments).

the *cpxA** mutation (Fig. 3A). As noted above (*7*), this mutation prevents jamming, as evidenced by the lack of accumulation of the precursor form of MalE in induced *cpxA** *lamB-lacZ* fusion strains (Fig. 3C). Overproduction of YccA alone was sufficient to prevent jamming in the *lamB-lacZ cpxA*$^{+}$ strain (Fig. 3C) and to prevent SecY destruction (Fig. 3B). The mutant YccA11 protein also stabilizes SecY (Fig. 3B). Thus, the toxicity associated with high-level production of LamB-LacZ is not entirely due to a physical jamming but rather is due, at least in part, to the proteolytic destruction of SecY.

YccA inhibits the protease FtsH (*13*). If this is the protease that degrades jammed SecY, then mutations that inactivate FtsH should result in hybrid protein secretion into the periplasm even better than do the *cpxA** mutations. Although the *ftsH* gene is essential, we could test this prediction using a strain that carries *sfhC21* (*14*). This allele suppresses the lethality of *ftsH* null but by itself does not dramatically alter the LacZ phenotype (fig. S2). Removing FtsH strongly reduced LacZ activity (Fig. 2), reflecting an enhanced secretion of LamB-LacZ to the periplasm.

SRP-mediated cotranslational secretion couples the processes of translation and translocation (Fig. 1) (*2*). Antibiotics that block translation elongation should produce proteins that are effectively fused to a ribosome by an unhydrolyzed, unreleased tRNA (*15*). We found that antibiotics that block translation elongation, such as chloramphenicol (Cm) and tetracycline (Tc), caused proteolytic destruction of SecY, whereas antibiotics that affect other stages of gene expression, such as translation initiation (kasugamycin) or transcription (rifamycin) did not (Fig. 4) (*11*). Furthermore, destruction of SecY upon treatment with Cm was FtsH-dependent (Fig. 4C). We have also investigated the fate of SecE and SecG. SecE was also degraded in the presence of Cm, although more slowly than SecY, whereas SecG was not (Fig. 4, C and D). Lastly, in agreement with the notion that SRP-dependent substrates define the target for FtsH-mediated translocon destruction upon treatment with antibiotics that inhibit translation elongation, high-level production of PhoA, a protein that is secreted in SRP-independent fashion, increased the stabililty of SecY upon treatment with Cm (fig. S3).

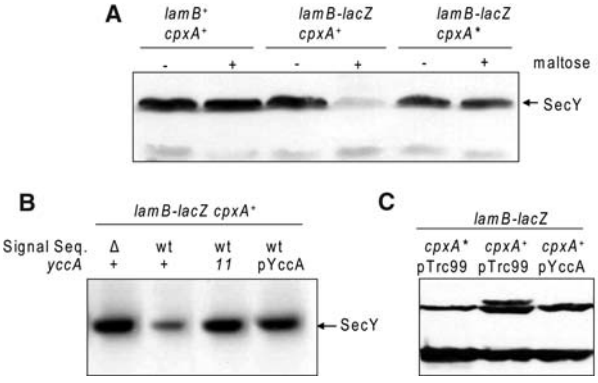

Fig. 3. Increased YccA stabilizes SecY and enables translocation of LamB-LacZ. (**A**) Immunoblot of SecY from strains carrying either wild-type *lamB* or the *lamB-lacZ* fusion and with either wild-type *cpxA* or the constitutive *cpxA** allele incubated in the presence (+) or absence (–) of maltose for 4 hours. (**B**) Immunoblot of SecY from strains incubated in the presence of maltose for 6 hours, of *cpxA*$^{+}$ strains carrying the *lamB-lacZ* fusion with (wt; Pop3186) and without (Δ; BZR60) its signal sequence, and expressing either endogenous levels of YccA (+), wild-type *yccA* on a multi-copy plasmid (pYccA), or the protease-resistant form of YccA (*yccA11*) from the chromosomal gene. (**C**) Immunoblot of MalE from cultures incubated in the presence of maltose for 1.5 hours. The empty vector (pTrc99a) and the *yccA* overexpression plasmid (pYccA) were induced with 2 μM IPTG 4 hours before and during induction with maltose.

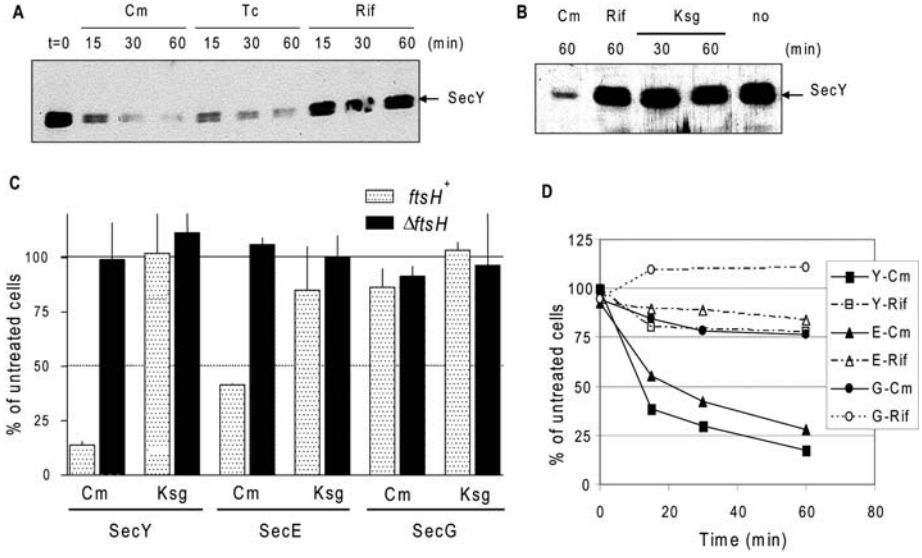

Fig. 4. Antibiotic inhibition of translation elongation results in SecY degradation. (**A**) Immunoblot of SecY from cultures untreated (t = 0) or incubated for the indicated times with 30 mg/L Cm, 10 mg/L Tc, or 100 mg/L rifampicin (Rif). (**B**) Immunoblot of SecY from cultures untreated (no) or incubated for the indicated times with 30 mg/L Cm, 100 mg/L Rif, or 200mg/L kasugamycin (Ksg). (**C**) Normalized levels of SecY, SecE, and SecG in an *ftsH*$^{+}$ strain (Pop3186, stippled bars) and an *ftsH* null strain (JVS679, solid bars), as determined by means of immunoblotting in cultures incubated for 30 min with Cm or Ksg. Values of untreated cultures have been set to 100%; each value is the mean of duplicate cultures, and the range is indicated. (**D**) The levels of SecY (squares), SecE (triangles), and SecG (circles) were determined by means of immunoblotting in cultures incubated for the indicated times with Cm (solid lines) or Rif (dashed lines).

Our results reveal a new activity for several old antibiotics. Because the secretion of many proteins occurs in a cotranslational fashion, agents that inhibit translation elongation will result in jammed translocators, and this will lead to the proteolytic destruction of these translocators. The suicidal nature of SecY destruction reflects the fact that SecY is required to insert newly synthesized SecY in the membrane (*16*). This chicken-and-the-egg–like problem may help explain why antibiotics that inhibit translation elongation exhibit bactericidal effects much sooner in some bacteria than in others (*17*, *18*). Perhaps the most susceptible bacteria have lower amounts of functional SecY.

We propose that *E. coli*, and perhaps all cells, have mechanisms that respond to SecY (or Sec61) translocators that are struggling with difficult substrates by degrading the stressed translocator. Clearly, such degradative activities can have dire consequences, and thus cells also have mechanisms to limit this suicidal activity. In *E. coli*, this limiting activity is controlled, at least in part, by the Cpx envelope stress response and YccA.

YccA is homologous to human Bax Inhibitor-1 (BI-1), an anti-apoptotic protein that restrains the activity of the tumor-suppressor Bax (*19*). BI-1 is so highly conserved that YccA from *E. coli* protects yeast cells against ectopically expressed human Bax (*20*). BI-1 is a proto-oncogene and is overexpressed in various types of cancer. Although Bax function is not fully understood, it contributes to cellular apoptosis caused by prolonged stress in the protein secretion pathway in eukaryotes (*21*), a pathway that involves the endoplasmic reticulum (ER) and is clearly related to the secretion stress caused by LacZ hybrids in bacteria. Moreover, Lisbona *et al.* (*22*) recently reported that BI-1 is a negative regulator of ER stress. Despite its obvious importance, the mechanism of action of BI-1 remains unknown, in part because of the inherent difficulty of studying the effects of Bax and its inhibitors in eukaryotic cells (*20*, *23*). Owing to the highly conserved function of BI-1 and YccA, studies of the bacterial counterpart may shed light on the mechanistic role of this important cell death regulator in human cells.

References and Notes

1. T. A. Rapoport, *Nature* **450**, 663 (2007).
2. R. S. Hegde, H. D. Bernstein, *Trends Biochem. Sci.* **31**, 563 (2006).
3. A. K. Veenendaal, C. van der Does, A. J. Driessen, *Biochim. Biophys. Acta* **1694**, 81 (2004).
4. C. W. Bowers, F. Lau, T. J. Silhavy, *J. Bacteriol.* **185**, 5697 (2003).
5. T. J. Silhavy, H. A. Shuman, J. Beckwith, M. Schwartz, *Proc. Natl. Acad. Sci. U.S.A.* **74**, 5411 (1977).
6. P. Bassford, T. J. Silhavy, J. Beckwith, *J. Bacteriol.* **139**, 19 (1979).
7. C. L. Cosma, P. N. Danese, J. H. Carlson, T. J. Silhavy, W. B. Snyder, *Mol. Microbiol.* **18**, 491 (1995).
8. W. B. Snyder, L. J. Davis, P. N. Danese, C. L. Cosma, T. J. Silhavy, *J. Bacteriol.* **177**, 4216 (1995).
9. N. L. Price, T. L. Raivio, *J. Bacteriol.* **191**, 1798 (2008).
10. K. Yamamoto, A. Ishihama, *Biosci. Biotechnol. Biochem.* **70**, 1688 (2006).
11. Materials and methods are available as supporting material on *Science* Online.
12. A. Kihara, Y. Akiyama, K. Ito, *Proc. Natl. Acad. Sci. U.S.A.* **92**, 4532 (1995).
13. A. Kihara, Y. Akiyama, K. Ito, *J. Mol. Biol.* **279**, 175 (1998).
14. T. Ogura *et al.*, *Mol. Microbiol.* **31**, 833 (1999).
15. C. Walsh, *Antibiotics: Actions, Origins, Resistance* (ASM Press, Washington, DC, 2003).
16. Y. Akiyama, K. Ito, *J. Biol. Chem.* **264**, 437 (1989).
17. W. E. Feldman, N. S. Manning, *Antimicrob. Agents Chemother.* **23**, 551 (1983).
18. J. J. Rahal Jr., M. S. Simberkoff, *Antimicrob. Agents Chemother.* **16**, 13 (1979).
19. Q. Xu, J. C. Reed, *Mol. Cell* **1**, 337 (1998).
20. H. J. Chae *et al.*, *Gene* **323**, 101 (2003).
21. M. I. Smith, M. Deshmukh, *Cell Death Differ.* **14**, 1011 (2007).
22. F. Lisbona *et al.*, *Mol. Cell* **33**, 679 (2009).
23. R. Huckelhoven, *Apoptosis* **9**, 299 (2004).

24. We thank I. Collinson for SecY antisera and T. Ogura for strains. This work was supported by the National Institute of General Medical Sciences (T.J.S.), the New Jersey Commission on Cancer Research (J.v.S.), and the Canton de Genève and the Swiss National Science Foundation (F.S. and D.B.).

Supporting Online Material

www.sciencemag.org/cgi/content/full/325/5941/753/DC1
Materials and Methods
Figs. S1 to S3
Table S1
References

12 February 2009; accepted 23 June 2009
10.1126/science.1172221

Synaptic Integration in Tuft Dendrites of Layer 5 Pyramidal Neurons: A New Unifying Principle

Matthew E. Larkum,[1]*† Thomas Nevian,[1]* Maya Sandler,[2] Alon Polsky,[2] Jackie Schiller[2]†

Tuft dendrites are the main target for feedback inputs innervating neocortical layer 5 pyramidal neurons, but their properties remain obscure. We report the existence of *N*-methyl-D-aspartate (NMDA) spikes in the fine distal tuft dendrites that otherwise did not support the initiation of calcium spikes. Both direct measurements and computer simulations showed that NMDA spikes are the dominant mechanism by which distal synaptic input leads to firing of the neuron and provide the substrate for complex parallel processing of top-down input arriving at the tuft. These data lead to a new unifying view of integration in pyramidal neurons in which all fine dendrites, basal and tuft, integrate inputs locally through the recruitment of NMDA receptor channels relative to the fixed apical calcium and axosomatic sodium integration points.

The pyramidal neuron is the basic computational unit of the cortex. Its distal tuft dendrite is heavily innervated by horizontal fibers coursing through layer 1 (L1), which provide long-range corticocortical and thalamocortical associational input (*1*–*6*). In the standard view of dendritic electrogenesis of L5 pyramidal neurons, the basal and apical tuft dendrites are quite different (*7*–*9*). Whereas thin basal dendrites of neocortical pyramidal neurons initiate local *N*-methyl-D-aspartate (NMDA) and weak Na^+ spikes (*10*–*12*), the apical dendrite is able to initiate calcium spikes (*13*–*17*). However, this view is based mostly on recordings from the thick apical dendrite, and little information is presently available with regard to the actual properties of the tuft dendrites, which are thin dendrites branching from the main bifurcation forming a tree that resembles more closely the basal dendritic tree. It has been suggested that the properties that give rise to calcium spikes are restricted to an apical band (*18*) beyond which the initiation of Ca^{2+} spikes becomes progressively more difficult (*19*) [but see Rhodes and Llinás (*20*)]. This raises questions about the active and passive properties of the tuft dendrites, which are vital to understanding how and where feedback inputs to the pyramidal neuron are integrated (*21*). To overcome the difficulties in recording from these fine dendrites, we combined two-photon excitation fluorescence microscopy and infrared-scanning gradient contrast (*10*).

Using multiple simultaneous patch-clamp recordings from near the main apical bifurcation point (658 ± 110 μm from the soma; $n = 28$) and secondary and tertiary/quaternary tuft branches (775 ± 98 μm from the soma, $n = 14$; and 859 ± 60, $n = 8$) to within 50 μm of the pia of L5 pyramidal neurons, we directly tested the local spiking capabilities of fine tuft dendrites. Recordings from higher-order branches mostly in L1 or near the border of L1/L2 are referred to as "distal tuft" recordings. We first investigated local integration of synaptic input using visually guided focal stimulation at preselected distal tuft dendrites while recording simultaneously the voltage from nearby locations (Fig. 1A). Recordings made from two distal tuft dendrites simultaneously while focally stimulating each of the branches revealed local, all-or-none spikes that failed to propagate to neighboring tuft branches (Fig. 1, B and C). On average, the spike attenuated by 86 ± 2.3% as it spread from one branch to another ($n = 3$).

Simultaneous recordings from distal and proximal tuft branches revealed that these all-or-none potentials originated in the fine distal tuft branches and attenuated as they spread proximally (Fig. 1, D to F). The voltage threshold for initiation of synaptically evoked dendritic spikes at the distal tuft branches was 9.67 ± 4.69 mV, and the amplitude of the spike at the distal tuft branch recording site was an additional 17.39 ± 5.87 mV from threshold and 27.07 ± 9.62 mV from baseline (*22*, *23*). These spikes attenuated further as they spread toward the main bifurcation point (by a factor of 2.25 ± 0.58; $n = 6$; average distance between the recording sites 189 ± 74 μm) (Fig. 1F) but still could contribute substantial depolarization. The cable-filtered distal tuft dendritic spike attenuated on average to 7.74 ± 2.8 mV at the proximal tuft recording site.

Because of their localization to the activated branch, we considered the possibility that, similar to basal dendrites, the main regenerative current of the distal tuft dendrites is carried through the synaptic currents themselves, that is, NMDA receptor channels (*11*). The specific NMDA receptor blocker AP5 (100 μM) completely abolished the dendritic spike and linearized the relationship between the synaptic stimulus intensity and the excitatory postsynaptic potential (EPSP) amplitude observed under control conditions ($n = 7$) (Fig. 1, G to I). To rule out the possibility that blockade of NMDA receptors simply increased the threshold for local spikes, we also used ultraviolet (UV) laser uncaging of glutamate (MNI-glutamate) directed to a specific location in the distal tuft dendrites while recording the nearby dendritic voltage (recordings at 832 ± 61.5 μm from the soma passed second bifurcation and mostly at third bifurcations; uncaging site was 18 ± 2.7 μm distal to recording site; $n = 8$) (Fig. 1J) (*24*). Gradually increasing the UV laser intensity evoked gradual EPSP-like potentials until a threshold value

[1]Department of Physiology, University of Berne, Bühlplatz 5, 3012 Berne, Switzerland. [2]Department of Physiology, The Rappaport Faculty of Medicine and Research Institute, Technion-Israel Institute of Technology, Bat-Galim, Haifa 31096, Israel.

*These authors contributed equally to this work.
†To whom correspondence should be addressed. E-mail: matthew.larkum@gmail.com (M.E.L.); jackie@tx.technion.ac.il (J.S.)